Article

Cell Reports

P-Rex1 Promotes Resistance to VEGF/VEGFR-Targeted Therapy in Prostate Cancer

Graphical Abstract

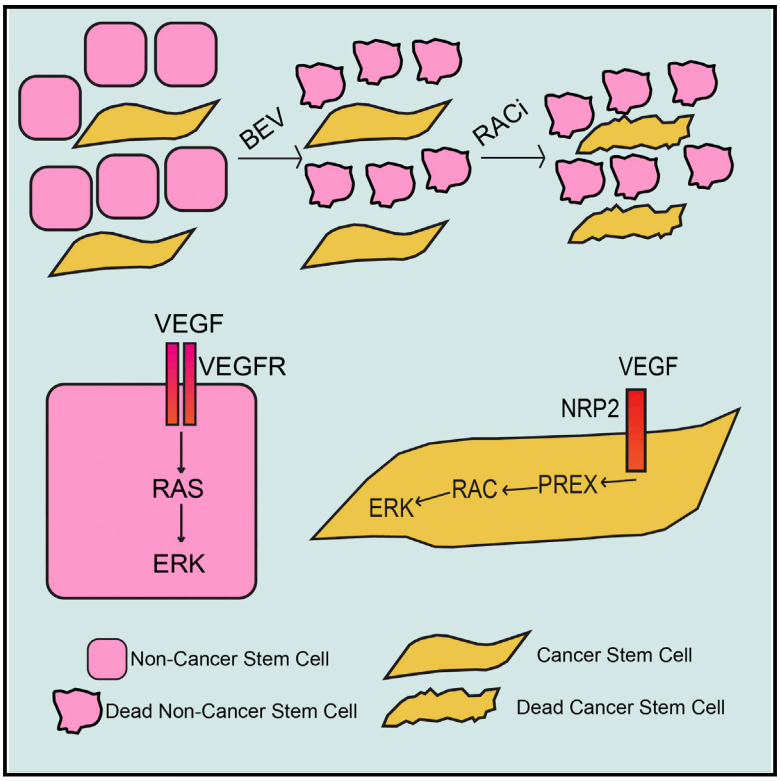

Highlights

- Prostate tumor cells resistant to bevacizumab have stem cell properties
- Resistance is mediated by VEGF/neuropilin signaling
- Neuropilin signaling induces P-Rex1 and activates Rac1, which sustains resistance
- Inhibition of P-Rex1 or Rac1 renders tumor cells sensitive to bevacizumab

Authors

Hira Lal Goel, Bryan Pursell, Leonard D. Shultz, Dale L. Greiner, Rolf A. Brekken, Craig W. Vander Kooi, Arthur M. Mercurio

Correspondence

hira.goel@umassmed.edu (H.L.G.), arthur.mercurio@umassmed.edu (A.M.M.)

In Brief

Understanding mechanisms of resistance to targeted therapy is critical. Goel et al. demonstrate that resistance to bevacizumab occurs by neuropilin signaling and activation of P-Rex1/Rac1. Inhibition of these molecules increases the sensitivity of prostate tumors to bevacizumab.

Goel et al., 2016, Cell Reports *14*, 2193–2208
March 8, 2016
http://dx.doi.org/10.1016/j.celrep.2016.02.016

CellPress

Cell Reports
Article

P-Rex1 Promotes Resistance to VEGF/VEGFR-Targeted Therapy in Prostate Cancer

Hira Lal Goel,[1,*] Bryan Pursell,[1] Leonard D. Shultz,[2] Dale L. Greiner,[3] Rolf A. Brekken,[4] Craig W. Vander Kooi,[5] and Arthur M. Mercurio[1,*]
[1]Department of Molecular, Cell and Cancer Biology, University of Massachusetts Medical School, Worcester, MA 01605, USA
[2]The Jackson Laboratory, Bar Harbor, ME 04609, USA
[3]Department of Molecular Medicine, University of Massachusetts Medical School, Worcester, MA 01605, USA
[4]Division of Surgical Oncology, Department of Surgery, Hamon Center for Therapeutic Oncology Research, University of Texas Southwestern Medical Center, Dallas, TX 75390, USA
[5]Department of Cellular and Molecular Biochemistry, Center for Structural Biology, University of Kentucky, Lexington, KY 40506, USA
*Correspondence: hira.goel@umassmed.edu (H.L.G.), arthur.mercurio@umassmed.edu (A.M.M.)
http://dx.doi.org/10.1016/j.celrep.2016.02.016

SUMMARY

Autocrine VEGF signaling is critical for sustaining prostate and other cancer stem cells (CSCs), and it is a potential therapeutic target, but we observed that CSCs isolated from prostate tumors are resistant to anti-VEGF (bevacizumab) and anti-VEGFR (sunitinib) therapy. Intriguingly, resistance is mediated by VEGF/neuropilin signaling, which is not inhibited by bevacizumab and sunitinib, and it involves the induction of P-Rex1, a Rac GEF, and consequent Rac1-mediated ERK activation. This induction of P-Rex1 is dependent on Myc. CSCs isolated from the PTEN$^{pc-/-}$ transgenic model of prostate cancer exhibit Rac1-dependent resistance to bevacizumab. Rac1 inhibition or P-Rex1 downregulation increases the sensitivity of prostate tumors to bevacizumab. These data reveal that prostate tumors harbor cells with stem cell properties that are resistant to inhibitors of VEGF/VEGFR signaling. Combining the use of available VEGF/VEGFR-targeted therapies with P-Rex1 or Rac1 inhibition should improve the efficacy of these therapies significantly.

INTRODUCTION

We are interested in the contribution of vascular endothelial growth factor (VEGF) and its receptors to prostate cancer and the potential for VEGF-targeted therapies in the treatment of this common cancer. Expression of VEGF is elevated in aggressive prostate cancer (Tomić et al., 2012), and a recent meta-analysis identified high VEGF expression as a prognostic factor for poor overall survival in men with prostate cancer (Wang et al., 2012). These and other data indicate that VEGF and VEGF receptors are feasible therapeutic targets. In fact, bevacizumab, a humanized VEGF antibody that blocks VEGF interactions with its tyrosine kinase receptors (VEGFRs) (Merino et al., 2011), and sunitinib, an inhibitor of VEGFRs and other receptors (Michaelson et al., 2014), have been used in clinical trials of prostate cancer patients (Merino et al., 2011). The prevailing assumption in these studies has been that these drugs target tumor angiogenesis (Merino et al., 2011; Goel and Mercurio, 2013). These trials did not yield a significant survival advantage, which has discouraged the use of these inhibitors for this disease. For example, the results from bevacizumab monotherapy were very disappointing, with no response noted based on RECIST (Response Evaluation Criteria in Solid Tumors) criteria, although 27% of patients exhibited a decline in prostate-specific antigen (Reese et al., 2001). A recent study of 873 patients with aggressive prostate cancer found that the addition of sunitinib to prednisone did not improve overall survival compared with placebo (Michaelson et al., 2014).

The reasons for the poor response to VEGF-targeted therapy in prostate cancer are not well understood but need to be considered in the context of the complexity of VEGF signaling in cancer. In addition to its contribution to endothelial biology and angiogenesis, VEGF signaling in tumor cells has emerged as an important factor in tumor initiation and progression (Goel and Mercurio, 2013; Chatterjee et al., 2013). More specifically, compelling evidence now exists that autocrine VEGF signaling is necessary for the function of cancer stem cells (CSCs) in prostate and other cancers (Goel and Mercurio, 2013; Goel et al., 2012). Given that CSCs have been implicated in resistance to therapy, tumor recurrence, and metastasis (Craft et al., 1999; Chen et al., 2013), this role for VEGF signaling is significant and it appears to be independent of its function as a mediator of tumor angiogenesis. The hypothesis can be formulated from this information that the poor response of prostate tumors, especially aggressive tumors, to anti-VEGF (bevacizumab) and anti-VEGR therapy is that these therapies do not target CSCs effectively despite the fact that they are dependent on VEGF signaling. In this study, we pursued this hypothesis and sought to investigate the mechanisms involved.

RESULTS

Cells with Stem-like Properties Are Resistant to Anti-VEGF/VEGFR Therapies

To assess the sensitivity of prostate CSCs to anti-VEGF therapy, we isolated a CD44^{+}CD24^{-} population from two freshly harvested

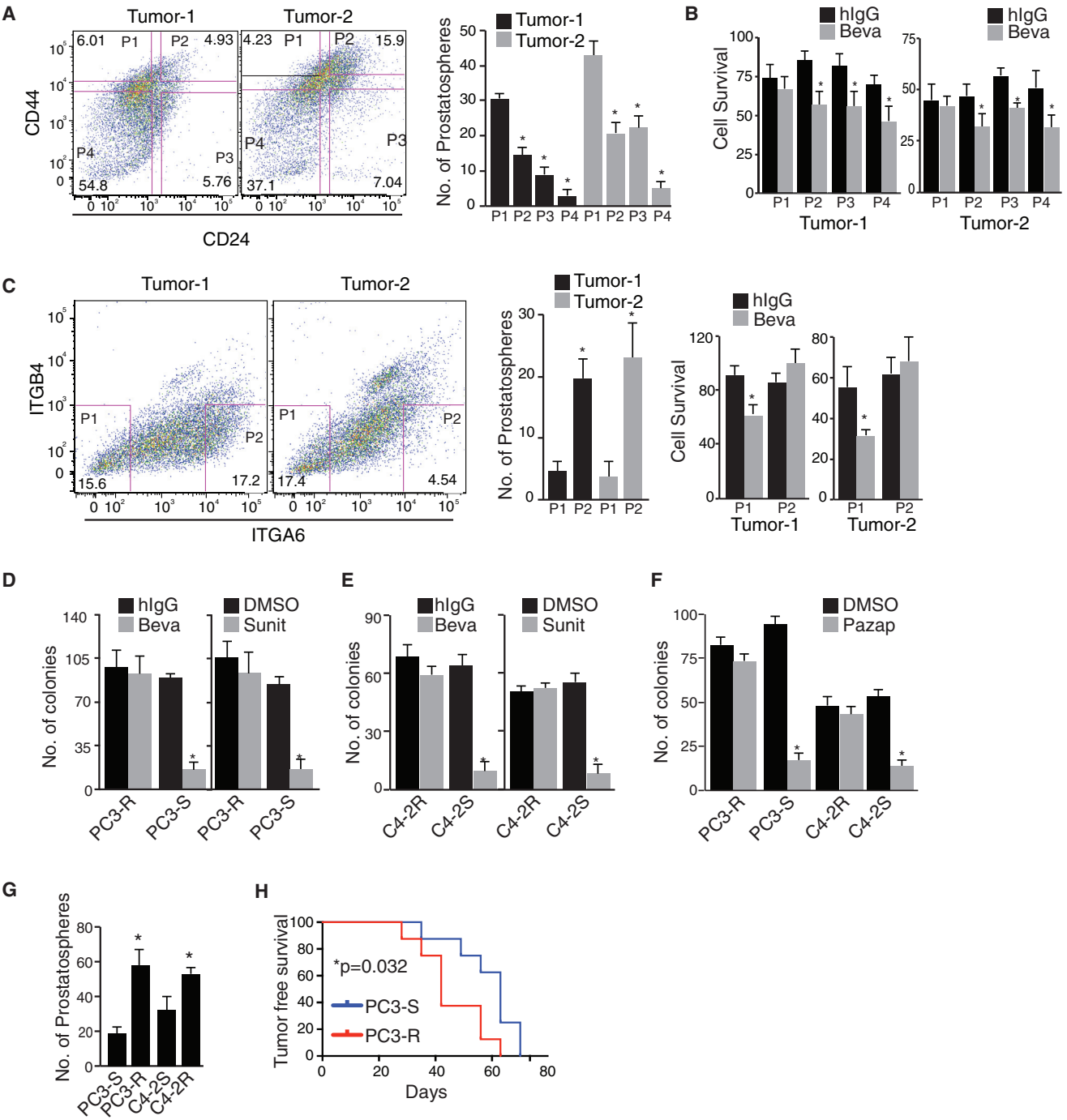

Figure 1. Characterization of Prostate Cancer Cells Resistant to VEGF-Targeted Therapy

(A and B) Cells from two human prostate tumors were sorted using CD44 and CD24 antibodies (A). The four subpopulations isolated based on expression of CD44 and CD24 were analyzed for their sensitivity to bevacizumab (B) and ability to form prostatospheres (A).

(C) Cells from two human freshly harvested prostate tumors were sorted using ITGA6 and ITGB4 antibodies. The four subpopulations isolated based on expression of ITGA6 and ITGB4 were analyzed for their ability to form prostatospheres and sensitivity to bevacizumab. For (B) and (C), the percentage of live cells in three different areas was determined and mean is plotted as cell survival.

(D and E) PC3 and C4-2 sensitive and resistant cells (1,000 cells per 60-mm plate) were cultured in the presence of bevacizumab (1 mg/ml), sunitinib (20 μM), or their respective controls for 10 days, colonies were stained with crystal violet, and colonies with more than 50 cells were counted.

(legend continued on next page)

human prostate tumors. This population is enriched for progenitor/stem cells (Hurt et al., 2008). Indeed, the $CD44^{+}CD24^{-}$ (P1) sub-population isolated from these tumors formed significantly more prostatospheres than the other sub-populations (Figure 1A), and it is the only subpopulation that exhibited resistance to bevacizumab treatment (Figure 1B). We also sorted these prostate tumors based on expression of CD49f (α6 integrin), another stem cell marker (Colombel et al., 2012), and observed that the high-CD49f population formed significantly more prostatospheres and exhibited resistance to bevacizumab treatment compared to the low-CD49f population (Figure 1C).

To understand the mechanism behind the resistance of CSCs to bevacizumab, we exposed prostate cancer cell lines (PC3 and C4-2) to increasing concentrations of bevacizumab until this inhibitor no longer affected their survival ($\sim$6 months). To circumvent VEGF-independent or transactivation of VEGFRs, we subsequently exposed these cells to increasing concentrations of sunitinib, an inhibitor of VEGRs and other VEGFRs (Michaelson et al., 2014), along with bevacizumab. However, sunitinib did not have a significant effect on bevacizumab-resistant cells (data not shown). The resistant cell lines generated are referred to as PC3-R and C4-2R. As controls, we also exposed these cell lines to control immunoglobulin G and DMSO and refer to these as sensitive cell lines (PC3-S and C4-2S) (Figures 1D and 1E).

Neither bevacizumab nor sunitinib inhibited the ability of the resistant cell lines to form colonies or survive, in contrast to the sensitive cell lines (Figures 1D, 1E, and S1A–S1D). Interestingly, PC3-R and C4-2R cells are also resistant to pazopanib, another VEGFR inhibitor (Figures 1F, S1E, and S1F), confirming the pathway specificity of the observed resistance. The resistant cell lines we generated are enriched for stem cell properties based on the fact that they were able to form prostatospheres and initiate tumors in NSG mice to a significantly greater extent than the sensitive cells (Figures 1G and 1H).

Neuropilin-Mediated Rac1 Activation Promotes Resistance to VEGF-Targeted Therapy

We compared the expression of key stem cell genes between the sensitive and resistant cell lines to substantiate our hypothesis that resistant cells exhibit stem cell properties. Indeed, the resistant cell lines are enriched in the expression of genes associated with CSCs (Nanog, Sox2, BMI1, and ALDH1) compared to the sensitive cell lines (Figure 2A). Interestingly, VEGF expression is markedly elevated in the resistant cell lines despite the fact that these cells were selected based on their resistance to bevacizumab. In contrast, no significant difference was observed in VEGFR2 expression between sensitive and resistant cells, and these cells lack expression of VEGFR1 (Figure 2A). Downregulation of VEGF expression in resistant cells reduced their ability to form colonies, suggesting that VEGF signaling contributes to bevacizumab and sunitinib resistance in a VEGFR2-independent manner (Figures S2A and S2B). The nature of this signaling was indicated by the observation that neuropilin (NRP) expression, especially NRP2, is dramatically elevated in resistant cell lines (Figures 2A and S2C). These expression data raised the possibility that VEGF/NRP signaling is responsible for resistance to bevacizumab and sunitinib, especially given the fact that bevacizumab blocks the interaction of VEGF with VEGFRs (VEGFR1–3), but not with NRPs (Geretti et al., 2010). The observation that IGF-1R expression is reduced dramatically in resistant cells (Figure 2A) is consistent with our previous finding that VEGF/NRP2 signaling represses IGF-1R transcription (Goel and Mercurio, 2013; Goel et al., 2012).

The contribution of NRPs to resistance was investigated using c-furSEMA, an inhibitory peptide, which blocks interactions of VEGF with NRPs (Parker et al., 2010). This peptide inhibited formation of prostatospheres in resistant cell lines and showed no effect in sensitive cells (Figure 2B). Importantly, treatment with c-furSEMA or an inhibitory NRP2 antibody decreased colony formation, highlighting a critical role for NRPs in the survival of resistant cells (Figure S2D). We also observed that inhibition of VEGF-NRP binding using c-furSEMA increased the sensitivity of resistant cells to bevacizumab, substantiating the critical function of NRPs in resistance to this VEGF inhibitor (Figure 2C). Furthermore, downregulation of either NRP2 or NRP1 significantly reduced colony formation and increased sensitivity to bevacizumab (Figure S2E). We focused on NRP2 for subsequent experiments based on our previous work (Goel and Mercurio, 2013; Goel et al., 2012) and the observation that NRP2 downregulation had a more potent inhibitory effect on colony formation than NRP1 (Figure S2E). Ectopic expression of NRP2 in sensitive cells induces resistance to bevacizumab in the presence of VEGF, directly implicating NRP2 in resistance to bevacizumab (Figure S2F).

Based on our finding that VEGF/NRP signaling promotes resistance to VEGF/VEGFR-targeted therapy, we investigated the details of this signaling mechanism. Initially, we compared activation of AKT and extracellular signal-regulated kinase (ERK) in sensitive and resistant cell lines, in the absence or presence of exogenous VEGF. Sensitive cells exhibited increased ERK activation in response to VEGF, which was inhibited by bevacizumab (Figure 2D). In contrast, resistant cells displayed relatively high ERK activation even in the absence of exogenous VEGF (Figure 2E), presumably the consequence of autocrine VEGF secretion in these cells. Interestingly, bevacizumab was unable to inhibit ERK activation in resistant cells (Figures 2F and 2G), suggesting that VEGF can induce ERK activation in these cells independently of VEGFR. No differences in AKT activation were observed between sensitive and resistant cells (Figures 2F and 2G). Since bevacizumab does not block the interaction of VEGF with NRP (Geretti et al., 2010), we expressed NRP2 in sensitive cells and observed that it induced ERK activation in the presence of bevacizumab (Figures 2H and 2I). This result implicates VEGF/NRP2 signaling in ERK activation. Interestingly, RAS does not appear to be involved in this mode of

(F) PC3- and C4-2-resistant and sensitive cell lines were analyzed for colony formation in the presence or absence of 10 μM pazopanib.
(G) Resistant and sensitive PC3 and C4-2 populations were compared for their ability to form prostatospheres.
(H) Resistant and sensitive PC3 populations were implanted into NSG mice, and tumor onset was plotted.
Error bars represent mean $\pm$ SD. Beva, bevacizumab; hIgG, control immunoglobulin G. See also Figure S1.

A

	C4-2S	C4-2R	PC3-S	PC3-R
STEMNESS				
OCT 4	1 (0.03)	0.98 (0.02)	1 (0.07)	3.3 (0.06)
Bmi-1	1 (0.03)	2.9 (0.042)	1 (0.05)	7.6 (0.43)
GLI1	1 (0.07)	4.2 (0.28)	1 (0.09)	8.5 (0.57)
KLF4	1 (0.21)	1.39 (0.09)	1 (0.08)	0.91 (0.18)
NANOG	1 (0.042)	3.1 (0.04)	1 (0.03)	15 (1.99)
SOX2	1 (0.17)	4.8 (0.139)	1 (0.42)	5.6 (0.84)
ALDH1	1 (0.46)	2.2 (0.68)	1 (0.19)	1.9 (0.48)
ALDH2	1 (0.8)	1.6 (0.6)	1 (0.23)	1.15 (0.63)
ALDH3	1 (0.02)	0.9 (0.45)	1 (0.02)	1.4 (0.8)
Snail1	1 (0.1)	1.6 (0.5)	1 (0.09)	2.6 (0.12)
VEGF	1 (0.05)	8.7 (0.2)	1 (0.03)	6.3 (0.7)
GROWTH FACTOR RECEPTOR				
c-Met	1 (0.13)	1.04 (0.36)	1 (0.037)	1.17 (0.42)
EGFR	1 (0.055)	0.5 (0.02)	1 (0.01)	3.6 (1.89)
IGF1R	1 (0.035)	0.12 (0.05)	1 (0.049)	0.18 (0.07)
IR	1 (0.04)	1.23 (0.52)	1 (0.15)	2.2 (1.11)
VEGFR1	0	0	0	0
VEGFR2	1.18 (0.68)	0.68 (0.12)	1 (0.23)	1.5 (0.58)
NPR1	1 (0.02)	6.3 (0.06)	1 (0.01)	6.11 (0.44)
NPR2	1 (0.042)	17.7 (1.56)	1 (0.27)	15.08 (1.99)

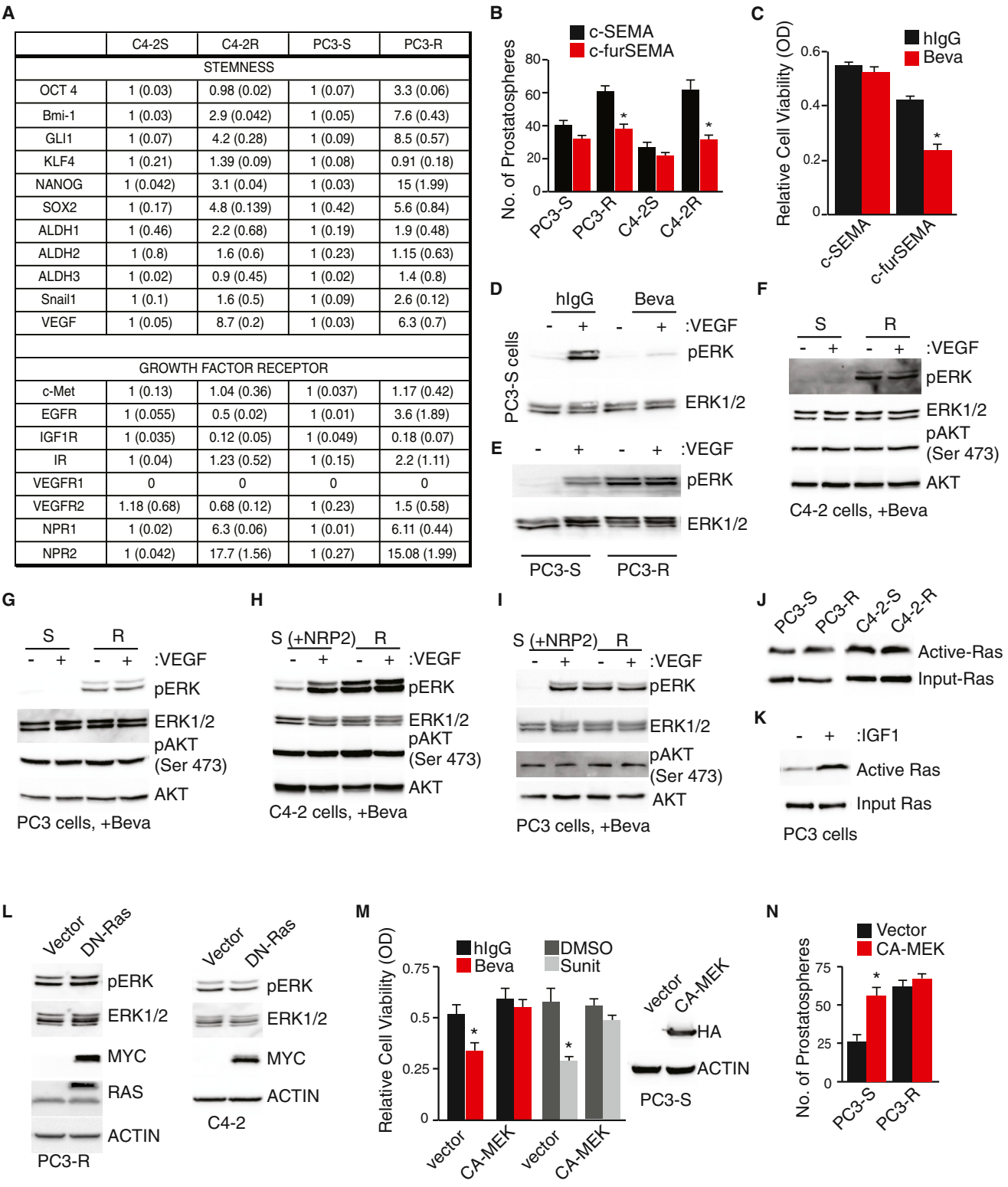

Figure 2. VEGF/NRP-Mediated Activation of ERK Promotes Resistance to Therapy

(A) Expression of CSC-related genes and growth factor receptors was quantified by qPCR in resistant and sensitive populations of PC3 and C42 cells. Tables show fold change in mRNA expression upon normalization with sensitive populations, which was set as 1.

(legend continued on next page)

ERK activation based on the findings that no differences in the levels of active RAS were detected between sensitive and resistant cells (Figures 2J and 2K) and that expression of a dominant-negative RAS (DN-RAS) did not alter ERK activation in resistant cells (Figure 2L). ERK activation contributes to resistance based on the finding that expression of constitutively active MEK in sensitive cells increased their resistance to bevacizumab and sunitinib-mediated inhibition of viability and prostatosphere formation (Figures 2M and 2N).

Subsequently, we focused on Rac1 as a mediator of Ras-independent ERK activation based on the reports that Rac1 is a major effector of NRP/plexin signaling (Liu and Strittmatter, 2001; Riccomagno et al., 2012) and plays a central role in vascular development in response to VEGF (Tan et al., 2008). Also, activation of Rac1 is associated with aggressive prostate cancer (Kobayashi et al., 2010), and $Rac1^{-/-}$ mice exhibit impaired ERK activation and regression of hematopoietic stem cells (Gu et al., 2003). Indeed, we found that resistant cell lines exhibit robust Rac1 activation compared to sensitive cells (Figure 3A). Rac1 mediates ERK activation in resistant cells based on the use of a dominant-negative Rac construct (Figure 3B). The activity of Rac1 in resistant cells is dependent upon NRP signaling because c-furSEMA reduced Rac1 activity significantly (Figure 3C). In contrast, addition of recombinant VEGF did not increase Rac1 activity or the ability of these cells to make prostatospheres (Figure 3D), most likely because resistant cells express high levels of autocrine VEGF (Figure 2A). This possibility was confirmed by depleting VEGF expression in these cells and observing a marked reduction in Rac1 activity (Figure 3E).

Sensitive cells may not respond to VEGF and activate Rac1 because they lack significant NRP expression. To test this possibility, we expressed either NRP1 or NRP2 in these cells and observed an increase in Rac1 activity and prostatosphere formation (Figure 3F). Also, expression of a constitutively active Rac1 in sensitive cells increased prostatosphere formation and expression of a dominant-negative Rac1 in resistant cells decreased their formation (Figure 3G). These results were confirmed using a Rac1 inhibitor (EHT1864) in resistant cells, which reduced the number of prostatospheres (Figure 3H). Although there is some indication that the ability of EHT1864 to inhibit Rac1 may be indirect (data not shown), we conclude from the use of dominant-negative and constitutively active Rac1 constructs, as well as EHT1864, that Rac1 is the primary mediator of VEGF/NRP-mediated prostatosphere formation.

To validate the role of Rac1 in tumor initiation, we utilized the $PTEN^{pc-/-}$ transgenic mouse model of prostate cancer (Mulholland et al., 2009). Tumors that form in this model harbor a small population of tumor initiating cells defined as $Lin^{-}Sca^{+}CD49f^{high}$ (referred to as $Lin^{-}Sca^{+}CD49f^{high}$ [LSC] cells) (Mulholland et al., 2009). We purified these LSC cells from 10-week-old $PTEN^{pc-/-}$ mice and observed increased expression of VEGF and NRP2 in this population compared to non-LSC cells (Figure S2G). We tested the hypothesis that Rac inhibition increases sensitivity to mcr84, which recognizes both mouse and human VEGF (Sullivan et al., 2010), and sunitinib. This antibody (mcr84) does not inhibit the interaction of VEGF with NRPs (Figure S2H). Consistent with our hypothesis, we observed that the Rac1 inhibitor increased the sensitivity of LSC cells to these drugs (Figure 3I). Inhibition of Rac1 also reduced the expression of VEGF, NRP2 and other stemness-related genes (Figure 3J).

The data in Figure 3I suggest that the response to VEGF-targeted therapy (bevacizumab or mcr84) would be improved significantly if Rac1 expression or activation were inhibited. To test this possibility initially, we treated control and Rac1-depleted PC3-R xenografts with bevacizumab or vehicle. Bevacizumab treatment alone had no significant effect on tumor growth, validating our in vitro finding that resistant cell lines can tolerate bevacizumab treatment. Although Rac1 inhibition reduced tumor volume, the combination of bevacizumab and Rac1 depletion resulted in a significantly better decrease in tumor volume (Figure 4A). Moreover, the residual tumors harvested from mice that received the combined treatment contained mostly apoptotic cells, in contrast to either bevacizumab treatment or Rac1 inhibition alone (Figure 4B). This unexpected observation suggests that resistant cells acquire sensitivity to bevacizumab as a result of Rac1 inhibition. Presumably, Rac1 inhibition alone reduces tumor growth but does not induce the massive apoptosis seen with combined treatment. To pursue this hypothesis further, $PTEN^{pc-/-}$ transgenic mice were treated with the Rac1 inhibitor (EHT1864), mcr84, or both at the start of puberty (6 weeks). Indeed, Rac1 inhibition reduced the number of LSC cells significantly but the combined treatment abolished the LSC population. We also compared the impact of mono- and

(B and C) Resistant and sensitive populations were analyzed for prostatosphere formation (B) or sensitivity to bevacizumab (1 mg/ml) (C) in the presence of either a NRP inhibitory peptide (c-furSEMA) or control peptide (c-SEMA).

(D) PC3-S cells were serum-deprived overnight and stimulated with VEGF (50 ng/ml) for 30 min in the presence or absence of bevacizumab (5 mg/ml). The activation of ERK was analyzed by immunoblotting using a phospho-specific antibody.

(E) PC3-sensitive or resistant cells were serum-deprived overnight and stimulated with VEGF (50 ng/ml) for 30 min. The activation of ERK was analyzed by immunoblotting using a phospho-specific antibody.

(F and G) Sensitive and resistant PC3 and C4-2 cell lines were serum-deprived overnight and stimulated with VEGF (50 ng/ml) for 30 min in the presence of bevacizumab (5 mg/ml). The activation of ERK and AKT was analyzed by immunoblotting using phospho-specific antibodies.

(H and I) NRP2 was expressed in sensitive populations of PC3 and C4-2 cells. These cells and resistant PC3 and C4-2 cells serum-deprived overnight and stimulated with VEGF (50 ng/ml) for 30 min in the presence of bevacizumab (5 mg/ml). The activation of ERK and AKT was analyzed by immunoblotting.

(J) Ras activation was analyzed in sensitive and resistant PC3 and C4-2 cell using the Raf1 binding assay.

(K) PC3-S cells were stimulated with IGF-1 (100 ng/ml) for 20 min and Ras activation was analyzed.

(L) Resistant PC3 and C4-2 cells were transfected with a Myc-tagged dominant-negative (DN) Ras construct, and ERK activation was analyzed by immunoblotting.

(M and N) Sensitive PC3 cells were transfected with a hemagglutinin (HA)-tagged, constitutively active (CA) MEK construct, and sensitivity to bevacizumab (M) and the effect on prostatosphere formation (N) were analyzed.

Error bars represent mean ± SD. Beva, bevacizumab; hIgG, control immunoglobulin G. See also Figure S2.

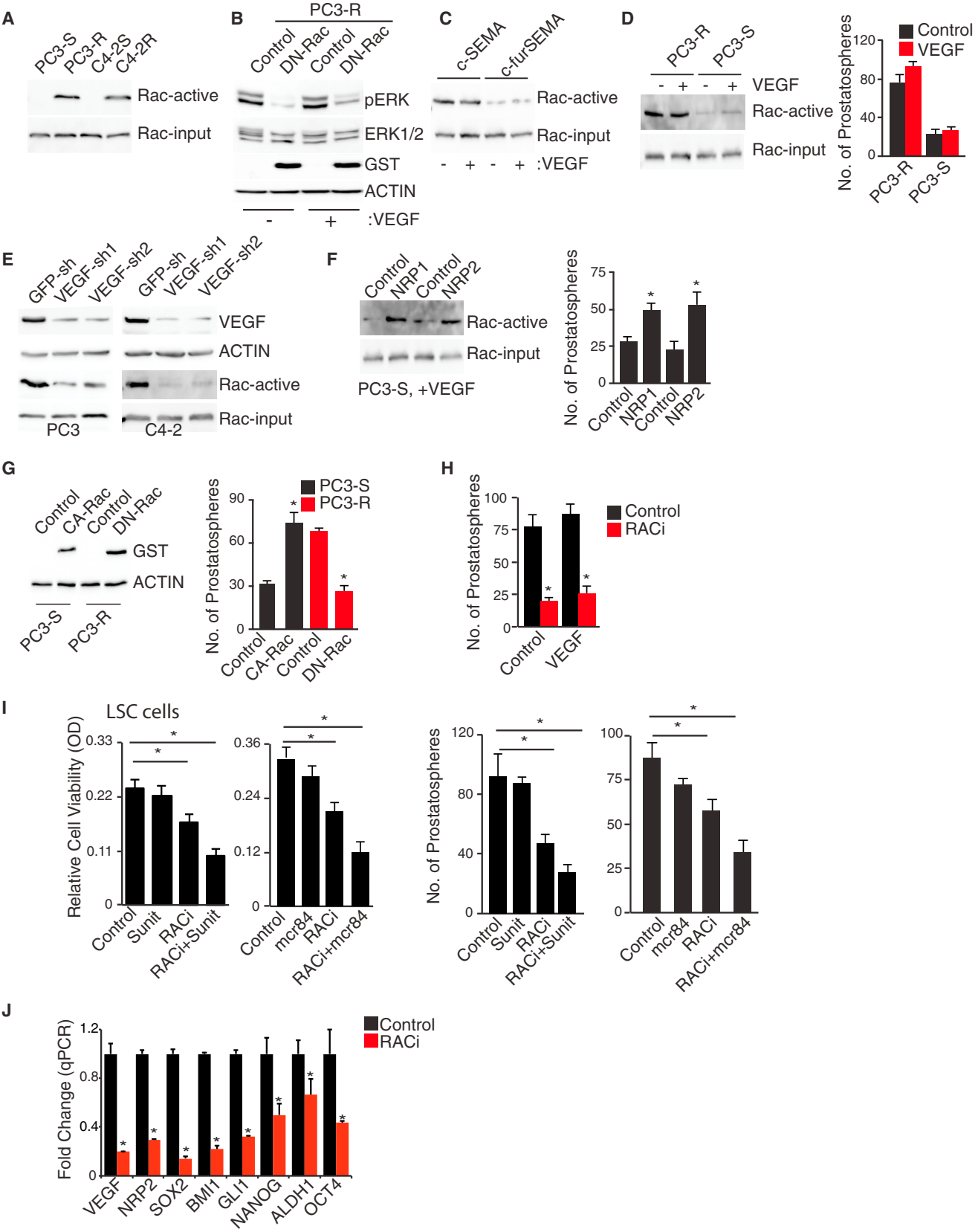

(legend on next page)

combined therapy on PTEN$^{pc-/-}$ tumors by calculating the weights of the isolated genitourinary (GU) tracts and prostate lobes. Combined treatment (EHT1864 + mcr84) resulted in a significant decrease in the weight of the isolated GU tracts and prostate lobes compared to either EHT1864 or mcr84 alone (Figures 4C and 4D). Pathological examination revealed that tumors progressed to well-differentiated adenocarcinomas in mice that received either control or single-agent treatment. Interestingly, however, prostatic intraepithelial neoplasia (PIN) lesions were observed in the prostate glands of mice that received combined treatment (RACi + mcr84), suggesting a delay in tumor progression as a result of the reduced number of LSC cells (Figure 4E). Moreover, a mass of cells in the lumen of the gland was evident in mice that received the combined treatment. Further analysis using the TUNEL assay demonstrated that this mass of cells is apoptotic, indicating that combined treatment can induce apoptotic cell death within PIN lesions (Figures 4F and S3). We also stained these tumor groups with CD31 and observed no significant difference in staining among the groups, indicating that the observed impact of these treatments is not caused by an effect of these compounds on angiogenesis (Figure S4A).

Identification of P-Rex1 as the Mediator of Resistance to VEGF-Targeted Therapy

To understand how VEGF/NRP signaling activates Rac1 and promotes resistance to VEGF/VEGFR-targeted therapy, we compared the expression of potential guanine-nucleotide exchange factors (GEFs) known to be involved in Rac1 activity in sensitive and resistant cells (Figure 5A). This screening revealed elevated expression of P-Rex1 and, to as lesser extent, TIAM1 in resistant cells (Figure 5A). The importance of P-Rex1 in Rac1 activation is indicated by our finding that expression of exogenous P-Rex1 in VEGF-depleted resistant cells or in sensitive cells restored Rac1 activation (Figures 5B and S4B). In contrast, downregulation of TIAM1 expression in resistant cells had no effect on Rac1 activation (Figure 5C), suggesting that endogenous P-Rex1 is sufficient to maintain Rac1 activation even in the absence of TIAM1. For this reason, we focused subsequent experiments on P-Rex1. P-Rex1 expression is dependent upon VEGF/NRP signaling because downregulation of VEGF significantly reduced P-Rex1 expression in resistant cells (Figure 5D) and expression of either NRP1 or NRP2 in sensitive cells increased P-Rex1 expression (Figure 5E). Moreover, depletion of P-Rex1 expression in resistant cells diminished Rac1 activity and prostatosphere formation (Figure 5F). The importance of P-Rex1 in promoting resistance is indicated by the finding that downregulation of P-Rex1 in resistant cells increased their sensitivity to bevacizumab and sunitinib (Figure 5G).

Our P-Rex1 experimental results were validated by analyzing the gene expression profiles of epithelial cells micro-dissected from benign prostates and tumor cells from Pten-null prostate carcinomas (Garcia et al., 2014). P-Rex1 expression is significantly elevated in cancer cells compared to benign epithelium ($p = 0.04$) (Figure 5H). We also compared the expression levels of Rac GEFs in LSC and non-LSC cells isolated from PTEN$^{pc-/-}$ prostate tumors. Among all of the GEFs analyzed, only P-Rex1 expression is increased significantly in LSC compared to non-LSC cells (Figure 5I). P-Rex1 expression is higher in prostate adenocarcinoma compared to non-cancerous tissues (Qin et al., 2009). More specifically, we observed that P-Rex1 expression correlates with tumor grade (Figure 5J), similar to NRP2 expression (Goel et al., 2012). In fact, a positive correlation between P-Rex1 and NRP2 expression was detected in a cohort of prostate tumors (Figure 5J).

To demonstrate that VEGF-induced tumor initiation is dependent upon Rac1 activation, we engineered PC3 cells to express GFP under control of the VEGF promoter. We sorted these cells and generated two distinct populations designated VEGF^{high} and VEGF^{low} (Figure 6A). VEGF^{high} cells form more colonies in soft agar and initiate tumors more rapidly than VEGF^{low} cells (Figures 6B and 6C). Similar to the resistant cell lines described above, VEGF^{high} cells express high levels of genes associated with CSCs, NRPs, and P-Rex1 (Figure 6D). Also, the VEGF^{high} cells are more resistant to bevacizumab and sunitinib compared to the VEGF^{low} cells (Figure 6E). VEGF induces ERK activation, which is inhibited by bevacizumab in VEGF^{low} cells (Figure 6F). In contrast, VEGF^{high} cells exhibit high basal ERK activation and this activation is resistant to bevacizumab (Figure 6F). VEGF^{high} cells also exhibited increased Rac1 activity compared

Figure 3. Rac1 Mediates Stem Cell Properties and Resistance to VEGF-Targeted Therapy

(A) Rac1 activation was compared in resistant and sensitive PC3 and C4-2 cells.

(B) Resistant PC3 cells were transfected with a glutathione S-transferase (GST)-tagged dominant-negative (DN) Rac1 construct and stimulated with VEGF, and activation of ERK was analyzed by immunoblotting. GST expression indicates the level of DN-Rac expression.

(C) Rac1 activation was measured in resistant PC3 cells in response to VEGF treatment in the presence of either a NRP inhibitory peptide (c-furSEMA) or control peptide (c-SEMA).

(D) Resistant and sensitive PC3 cells were stimulated with VEGF and the effect on Rac1 activation and prostatosphere formation was measured.

(E) VEGF expression was diminished in resistant PC3 and C4-2 cells using two different shRNAs and the effect on Rac1 activation was determined.

(F) Either NRP1 or NRP2 was expressed in sensitive PC3 cells. These cells were stimulated with VEGF (50 ng/ml) for 30 min and the effect on Rac1 activation and prostatosphere formation was measured.

(G) Resistant and sensitive PC3 cells were transfected with a GST-tagged, dominant-negative Rac construct (DN-Rac) or a constitutively active Rac construct (CA-Rac), and their effect on prostatosphere formation was measured.

(H) PC3-R cells were stimulated with VEGF in the presence or absence of a Rac1 inhibitor (EHT1864; 20 μM) and the effect on prostatosphere formation was measured.

(I) Freshly sorted LSC cells from PTEN$^{pc-/-}$ mice were used to measure the effect of EHT1864, mcr84, or sunitinib on cell proliferation and prostatosphere formation.

(J) Freshly sorted LSC cells from PTEN$^{pc-/-}$ mice were treated with EHT1864 (20 μM), and expression of genes associated with stem cells and VEGF signaling was quantified by qPCR.

Error bars represent mean ± SD.

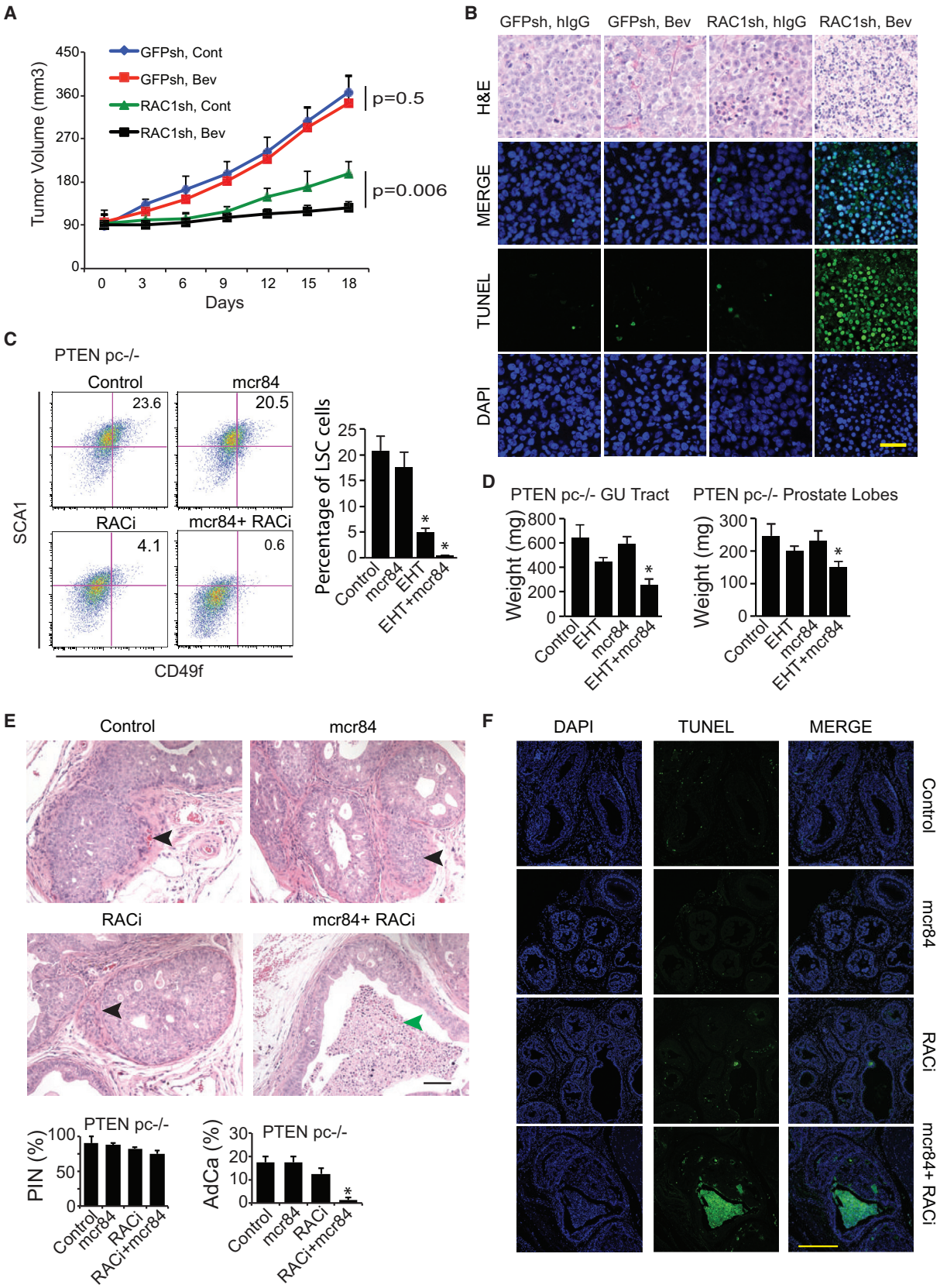

(legend on next page)

to the VEGF^{low} cells (Figure 6G). Also, downregulation of NRP2 in VEGF^{high} cells reduced Rac1 activation (Figure 6H). Importantly, inhibition of Rac1 in VEGF^{high} cells reduced their ability to form prostatospheres in vitro and tumors in vivo (Figures 6I and 6J). Also, P-Rex1 downregulation reduced tumor onset in vivo (Figure 6K), confirming the crucial role of P-Rex1 in VEGF/NRP/Rac1 signaling. Taken together, these data substantiate the ability of VEGF/NRP2/P-Rex1 signaling to activate Rac1 and the importance of this pathway in tumor formation.

To identify the mechanism of P-Rex1 regulation, we focused on its transcriptional regulation, because we observed increased activity of a luciferase reporter construct containing the P-Rex1 promoter in resistant cells compared to sensitive cells (Figure 7A). We used the UCSC genome browser to search for putative transcription factor binding sites on the P-Rex1 promoter and identified Myc as a possible candidate. A role for Myc is supported by the increased expression of Myc in resistant compared to sensitive cell lines, as well as enrichment of Myc-positive cells in PTEN$^{pc-/-}$ tumors upon treatment with mcr84 (Figures 7B and 7C). Moreover, Myc downregulation reduced Rac1 activation and P-Rex1 expression in resistant cells (Figures 7D, 7E, S5A, and S5B). More definitively, we detected direct binding of Myc on the P-Rex1 promoter by ChIP (Figure 7F), and mutation of a putative myc-binding site (CACTTG, −246) significantly reduced the activity of a luciferase promoter construct (Figure S5C). We also found a significant correlation in P-Rex1 and Myc expression in human prostate cancer specimens by immunohistochemistry (Figures 7G and S5D). These results infer that VEGF/NRP regulation of P-Rex1 is Myc dependent. Indeed, we observed that VEGF was unable to induce P-Rex1 expression in the presence of Myc small hairpin RNA (shRNA) in PC3-S cells engineered to express NRP2 (Figure 7E). Expression of Myc is VEGF dependent based on the findings that downregulation of VEGF reduced Myc expression and addition of VEGF increased Myc expression (Figures 7B and 7E).

Myc is a regulator of prostate cancer and prostate-specific expression of a Myc transgene drives carcinogenesis in a stepwise fashion from PIN to invasive cancer (Ellwood-Yen et al., 2003). Myc-Cap cells were derived from this transgenic mouse model. Inhibition of Rac1 in Myc-CaP cells reduced their ability to form colonies in soft agar (Figure 7H). Moreover, downregulation of Rac1 or P-Rex-1 expression significantly increased tumor-free survival in vivo, establishing the important role of Rac1/P-Rex1 in Myc-induced tumorigenesis (Figures 7I–7K).

DISCUSSION

This study was predicated on the results from clinical trials concluding that bevacizumab and VEGF receptor tyrosine kinase inhibitors are not effective therapies for prostate cancer (Merino et al., 2011). It is widely assumed that these drugs target tumor angiogenesis (Merino et al., 2011) and, consequently, the poor response observed in these clinical trials could be considered in the context of angiogenesis and the role of angiogenesis in prostate cancer. In contrast to this prevailing idea, we focused on the hypothesis that VEGF signaling in tumor cells, especially cells with stem-like properties, is critical for tumor propagation and progression and that this signaling, mediated primarily by NRPs, is a prime target for therapy (Goel and Mercurio, 2013). Indeed, the results we report demonstrate that prostate cancer cells selected for their resistance to bevacizumab and sunitinib are enriched for stem cell properties and NRP signaling. Most importantly, we demonstrate that NRP signaling induces expression of P-Rex1, a Rac1 GEF, and that Rac1-mediated ERK activation is responsible for resistance to bevacizumab and sunitinib. These findings reveal a role for VEGF/NRP-mediated regulation of P-Rex1 in the biology of CSCs and resistance to therapy.

An intriguing aspect of our study is the "VEGF paradox." Specifically, we observed that resistance to VEGF-targeted therapy (bevacizumab and sunitinib) is mediated by an enhancement of VEGF/NRP signaling. In fact, prostate cancer cells treated with bevacizumab and sunitinib exhibit a marked increase in VEGF expression despite the fact that bevacizumab targets the interaction of VEGF with VEGFRs (Ferrara, 2005). Our interpretation of these data is that neither bevacizumab nor sunitinib is effective at targeting prostate cancer cells with stem cell properties and that the CSC population, which is characterized by autocrine VEGF/NRP signaling, is enriched by treatment with these drugs because they target primarily non-CSCs. This hypothesis is supported by several studies that have highlighted the importance of VEGF/NRP signaling in CSCs and discounted the contribution of VEGFRs (Goel and Mercurio, 2013). In light of our data that resistant cells show lack of VEGF2 surface expression, we propose that NRP2-mediated VEGF signaling is independent of its role as a co-receptor for VEGFRs. This hypothesis is consistent with previous reports that VEGF/NRP signaling can occur independently of VEGFRs (Goel and Mercurio, 2013; Cao et al., 2013). Moreover, our previous observation that NRP2 associates with the α6β1 integrin and regulates CSC properties by activating focal adhesion kinase (FAK) (Goel et al., 2012, 2013)

Figure 4. Rac1 Inhibition Improves Sensitivity to VEGF-Targeted Therapy

(A) PC3-R cells were transfected with Rac1 shRNAs, and these cells were implanted in NSG mice. Once tumors reached ~100 mm^3 in volume, mice were treated with either control immunoglobulin G (Cont) or bevacizumab (Bev; 10 mg/kg, intraperitoneally [i.p.], twice weekly). Tumor volume was measured every third day.

(B) Control and treated PC3-R xenograft tumors were harvested, and apoptosis was analyzed using TUNEL staining. Scale bar, 10 μm.

(C and D) Six-week old PTEN$^{pc-/-}$ mice were injected i.p. with either mcr84 (10 mg/kg) or EHT1864 (10 mg/kg) twice weekly for 3 weeks. The GU tract was harvested, and total weight was measured. The prostate glands were separated and combined weight of all the lobes was measured. The prostate glands were digested, and LSC cells (Lin$^-$Sca$^+$CD49f^{high}) were isolated by fluorescence-activated cell sorting. The number of LSC cells is significantly reduced in mice treated with RACi or RACi+mcr84.

(E) H&E staining of prostate tumors from PTEN$^{pc-/-}$ mice described in (C). The percentage of prostate glands showing either PIN or well-differentiated adenocarcinoma (AdCa) was quantified as shown. Scale bar, 100 μm.

(F) Tumor sections of prostate tumors from PTEN$^{pc-/-}$ mice described in (C) were stained using the TUNEL reagent to detect apoptosis. Scale bar, 100 μm.

Error bars represent mean ± SD. Bev, bevacizumab; hIgG, control immunoglobulin G. See also Figures S3 and S4.

A

	C4-2S	C4-2R	PC3-S	PC3-R
	GEFs			
SOS1	1 (0.46)	0.99 (0.34)	1 (0.01)	1 (0.11)
P-Rex1	1 (0.065)	13.6 (2.3)	1 (0.046)	16.5 (0.48)
VAV1	1 (0.41)	1 (0.21)	1.02 (0.3)	1.09 (0.37)
VAV2	1 (0.29)	1 (0.21)	1 (0.07)	1 (0.36)
VAV3	1 (0.1)	1.2 (0.54)	1 (0.07)	1 (0.3)
TIAM1	1 (0.1)	6 (2.2)	1 (0..034)	8.7 (0.95)

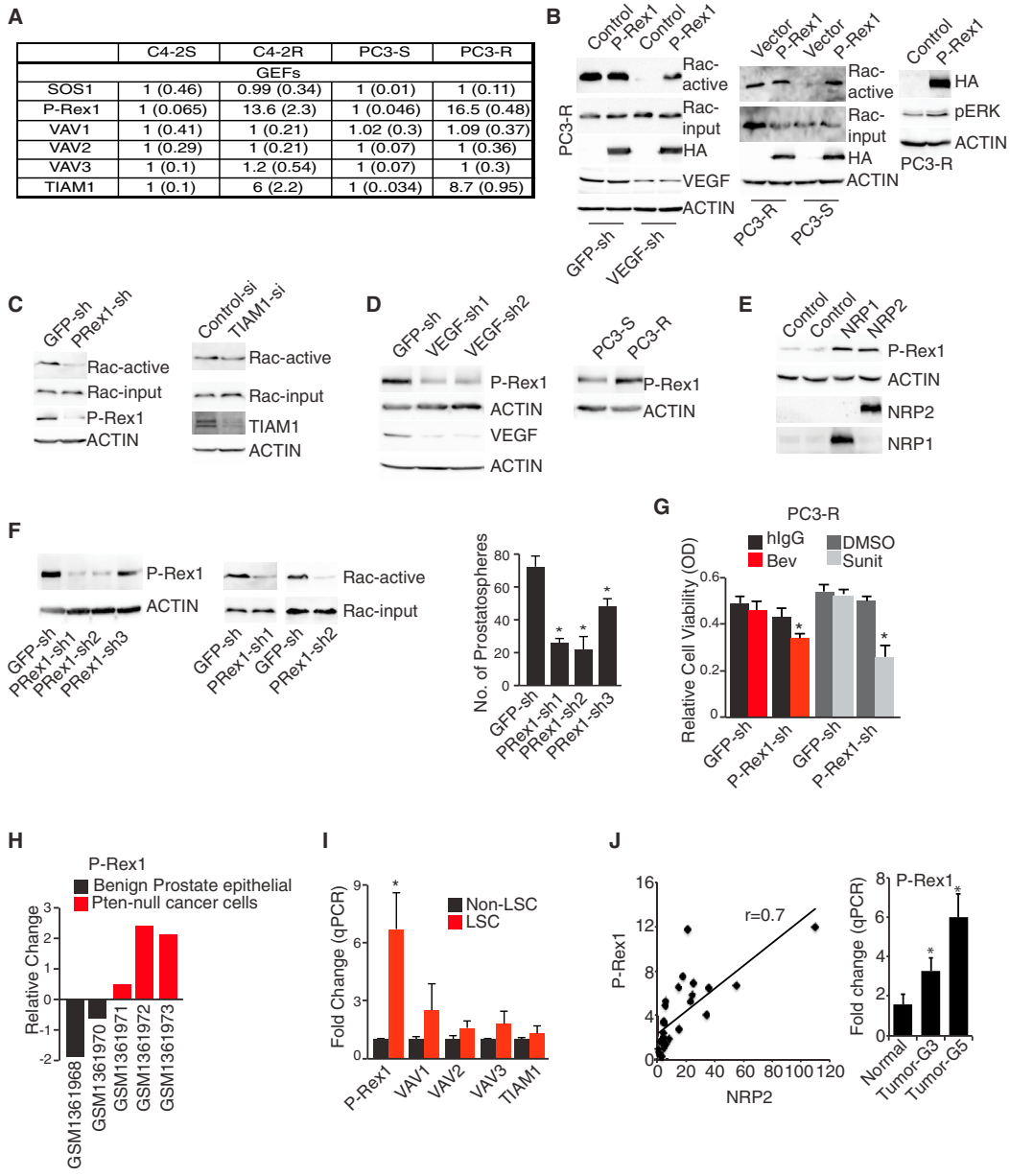

Figure 5. P-Rex1, a GEF, Promotes Rac1 Activation and Resistance to VEGF-Targeted Therapy

(A) The expression of Rac1 GEFs was compared in sensitive and resistant PC3 and C4-2 cell lines using qPCR. Table shows fold change in mRNA expression upon normalization with sensitive populations, which was set as 1.

(B) P-Rex1 was expressed in resistant PC3 cells in which VEGF expression had been diminished using shRNA and the effect on Rac activation was determined (left). P-Rex1 was expressed in resistant and sensitive PC3 cells and the effect on Rac activation was determined (middle). Right panels show the expression of HA-tagged P-Rex1 in PC3-R cells.

(C) Resistant PC3 cells were transfected with either P-Rex1 shRNA or TIAM1 siRNA, and the effect on Rac activation was determined.

(D) Protein extracts from resistant PC3 cells in which VEGF expression had been diminished using shRNA were immunoblotted with P-Rex1, VEGF, or actin antibodies.

(E) Either NRP1 or NRP2 was expressed in sensitive PC3 cells, and the effect on P-Rex1 expression was assessed by immunoblotting.

(F) Resistant PC3 cells were transfected with P-Rex1 shRNA, and the effect on prostatosphere formation and Rac1 activation was analyzed.

(G) Resistant PC3 cells expressing P-Rex1 shRNA were treated with bevacizumab (Bev; 1 mg/ml) or sunitinib (Sunit; 20 μM), and their proliferation was assayed. Beva, bevacizumab; hIgG, control immunoglobulin G.

(H) Expression of P-Rex1 was analyzed in a published dataset (GEO: GSE56469).

(I). Freshly harvested LSC cells from 9-week-old $PTEN^{pc-/-}$ mice were analyzed for expression of GEFs using qPCR.

(J) Expression of NRP2 and P-Rex1 mRNA was quantified by qPCR in microdissected sections from benign glands, as well as grade 3 and grade 5 prostate cancer specimens. A significant correlation (p value is 1×10^{-6}) in the expression of P-Rex1 and NRP2 was observed (r = 0.7).

Error bars represent mean ± SD.

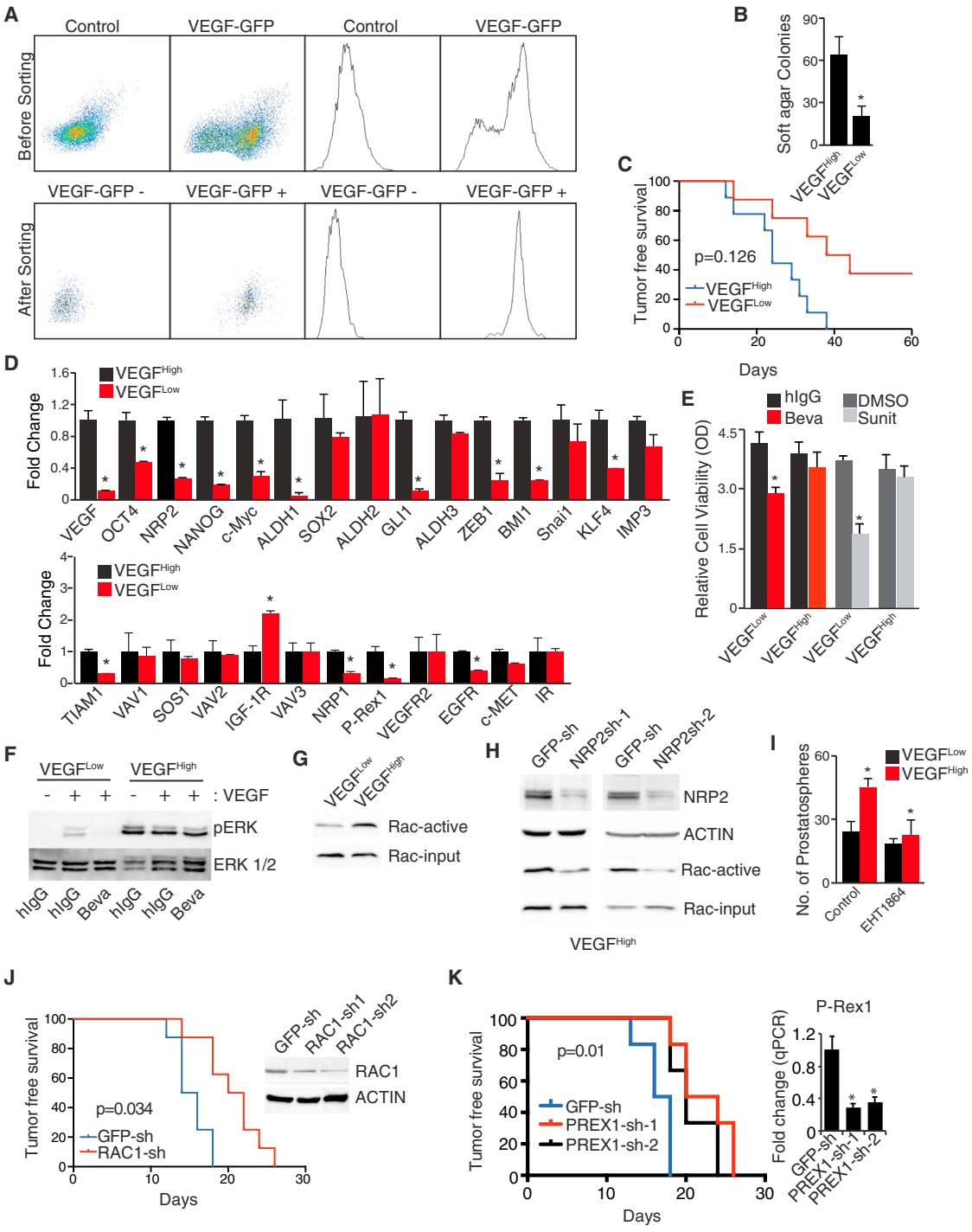

Figure 6. Rac1 Is Required for VEGF-Mediated Tumor Initiation

(A) PC3 cells were transfected with a GFP-expressing plasmid under control by the VEGF promoter and these cells were sorted based on their expression of GFP. The top panels show fluorescence-activated cell sorting (FACS) profile before GFP sorting, and the bottom panels show FACS profile after sorting.

(B) The ability of VEGF^{high} and VEGF^{low} cells to form colonies in soft agar was determined.

(C) VEGF^{high} and VEGF^{low} cells were implanted in NSG mice and tumor formation was detected by palpation.

(D) Expression of genes associated with stem cells and VEGF signaling was quantified by qPCR.

(E) VEGF^{high} and VEGF^{low} cells were incubated with bevacizumab (Bev; 1 mg/ml) or sunitinib (Sunit; 20 μM) for 72 hr, and their proliferation was assayed. Beva, bevacizumab; hIgG, control immunoglobulin G.

(legend continued on next page)

provides a potential mechanism for VEGF signaling that is independent of VEGFRs because FAK is known to mediate ERK activation (Zhao and Guan, 2009) and is important for CSCs (Luo et al., 2009).

Our data reveal an unexpected role for P-Rex1 and Rac1 activation in the genesis of prostate CSCs and resistance to bevacizumab and sunitinib. P-Rex1 is quite interesting in this regard because its expression is low in normal prostate and elevated in metastatic disease (Qin et al., 2009). There is also evidence that P-Rex1 can promote metastasis in a xenograft model of prostate cancer (Qin et al., 2009). Although many studies have implicated Rac1 in migration, invasion, initiation, and growth of tumor cells, including prostate cancer (Bid et al., 2013; Baker et al., 2014), our results show that P-Rex1-mediated Rac1 activation is critical for the formation and function of prostate CSCs. This conclusion is demonstrated most rigorously by our observation that treatment of mice harboring $PTEN^{pc-/-}$ tumors with a Rac1 inhibitor significantly reduced the number of LSC cells, which have been characterized as CSCs in this transgenic model (Mulholland et al., 2009). Also, treatment of these mice with the Rac1 inhibitor reduced the frequency of tumor formation, consistent with a role for Rac1 in the function of CSCs. We also provide evidence that Rac1-mediated activation of ERK is responsible for resistance to bevacizumab and sunitinib.

We provide mechanistic insight into the regulation of P-Rex1 expression by identifying Myc as a regulator of P-Rex1 transcription in prostate CSCs. This finding is relevant because Myc is significantly elevated in prostate CSCs compared to non-CSCs (Civenni et al., 2013). Also, gene set enrichment analysis of two independent datasets revealed that Myc expression is associated with tumor cells enriched with an embryonic stem cell-like gene signature (Civenni et al., 2013). Our data also indicate that VEGF/NRP signaling contributes to the regulation of Myc expression and Myc-induction of P-Rex1. This conclusion is supported by the report that VEGF/VEGFR2 signaling induces Myc expression in breast cancer cells by a mechanism that involves Stat 3 (Zhao et al., 2015). Based on our data, however, VEGF induction of Myc appears to be independent of VEGFRs. In this direction, we reported that VEGF/NRP signaling activates FAK in CSCs. (Goel et al., 2012, 2013). This observation is interesting based on the report that FAK regulates Myc transcription in epidermal stem cells (Ridgway et al., 2012). It is also worth noting that epigenetic repression of P-Rex1 in non-aggressive prostate cancer cell lines has been observed (Wong et al., 2011). However, our initial experiments suggested that epigenetic regulation does not account for the marked increase in P-Rex1 mRNA expression in PC3-R cells compared to PC3-S (Figure S6A).

An important question that arises from our data is how P-Rex1-mediated Rac1 activation impacts the function of prostate CSCs and promotes resistance to therapy. We posit that P-Rex1/Rac1-mediated ERK activation sustains the expression of VEGF and NRP2 and the ability of VEGF/NRP2 signaling to enhance the expression of BMI-1 and other stem cell factors. In essence, we suggest that p-Rex1/Rac1-mediated ERK activation contributes to a positive feedback loop involving VEGF/NRP2 signaling that sustains stem cell properties in prostate cancer. In addition, our previous work demonstrated that VEGF/NRP2 signaling contributes to ERK-mediated induction of Gli1 and BMI-1 expression and that this pathway can feedback to sustain NRP2 expression (Goel et al., 2013). These findings should be discussed in the context of a recent report concluding that autocrine semaphorin 3C promotes the survival of glioma stem cells by activating Rac1/nuclear factor κB signaling (Man et al., 2014). In contrast to our results, however, they observed that semaphorin-3C-mediated Rac1 activation does not impact ERK activation or the expression of stem cell factors. We also analyzed the expression of semaphorin 3C and targets of nuclear factor κB signaling and found no difference between sensitive and resistant populations (Figures S6B–S6D). Clearly, the available data indicate that Rac1 can affect the function of CSCs by distinct mechanisms that may relate to the biology of specific cancers. It is also worth noting that both semaphorin 3C and VEGF are ligands for NRP2, and an important aspect of our work is that we implicate VEGF-mediated activation of P-Rex1/Rac1 in resistance to bevacizumab, which has significant therapeutic implications. Interestingly, in this context, our analysis of gene profiling of metastatic colon cancer patients treated with bevacizumab revealed that high P-Rex1 or Myc expression is a significant predictor of poor progression-free survival (Figure S6E) (Pentheroudakis et al., 2014). Also, the analysis of gene expression in human glioblastoma xenografts treated with bevacizumab indicated increased expression of P-Rex1 and NRP2 (Figure S6F). Unfortunately, it is not possible to perform a similar analysis of prostate cancer patients treated with either bevacizumab or sunitinib (Michaelson et al., 2014; Kelly et al., 2012) because tumor specimens were not collected as an endpoint in these clinical trials (W.K. Kelly and M.D. Michaelson, personal communication).

Our data raise the exciting possibility that bevacizumab or VEGFR-targeted therapy in prostate cancer could be efficacious if it were combined with targeted inhibition of P-Rex1/Rac1. This possibility is supported by the data presented in Figures 4A and 6K. It is also timely and significant because there are few therapeutic options available for men with aggressive prostate cancer, which is enriched with tumor cells with a stem-like phenotype (Chen et al., 2013). Potent Rac1 inhibitors are available (Montalvo-Ortiz et al., 2012), but some concern is noted with their potential side effects as indicated by the reduced weight

(F) $VEGF^{high}$ and $VEGF^{low}$ cells were serum-deprived overnight and stimulated with VEGF (50 ng/ml) for 30 min in the presence or absence of bevacizumab (5 mg/ml). The activation of ERK was analyzed by immunoblotting using a phospho-specific antibody.
(G) Rac1 activation was compared in $VEGF^{high}$ and $VEGF^{low}$ cells.
(H) NRP2 expression in $VEGF^{high}$ cells was downregulated using shRNA, and Rac1 activation was assayed.
(I) Prostatosphere formation by $VEGF^{high}$ cells in the presence or absence of EHT1864 was quantified.
(J and K) $VEGF^{high}$ cells were transfected with shRNAs targeting either Rac1 (J) or P-Rex1 (K), and these cells were implanted in NSG mice. Tumor formation was detected by palpation.
Error bars represent mean ± SD.

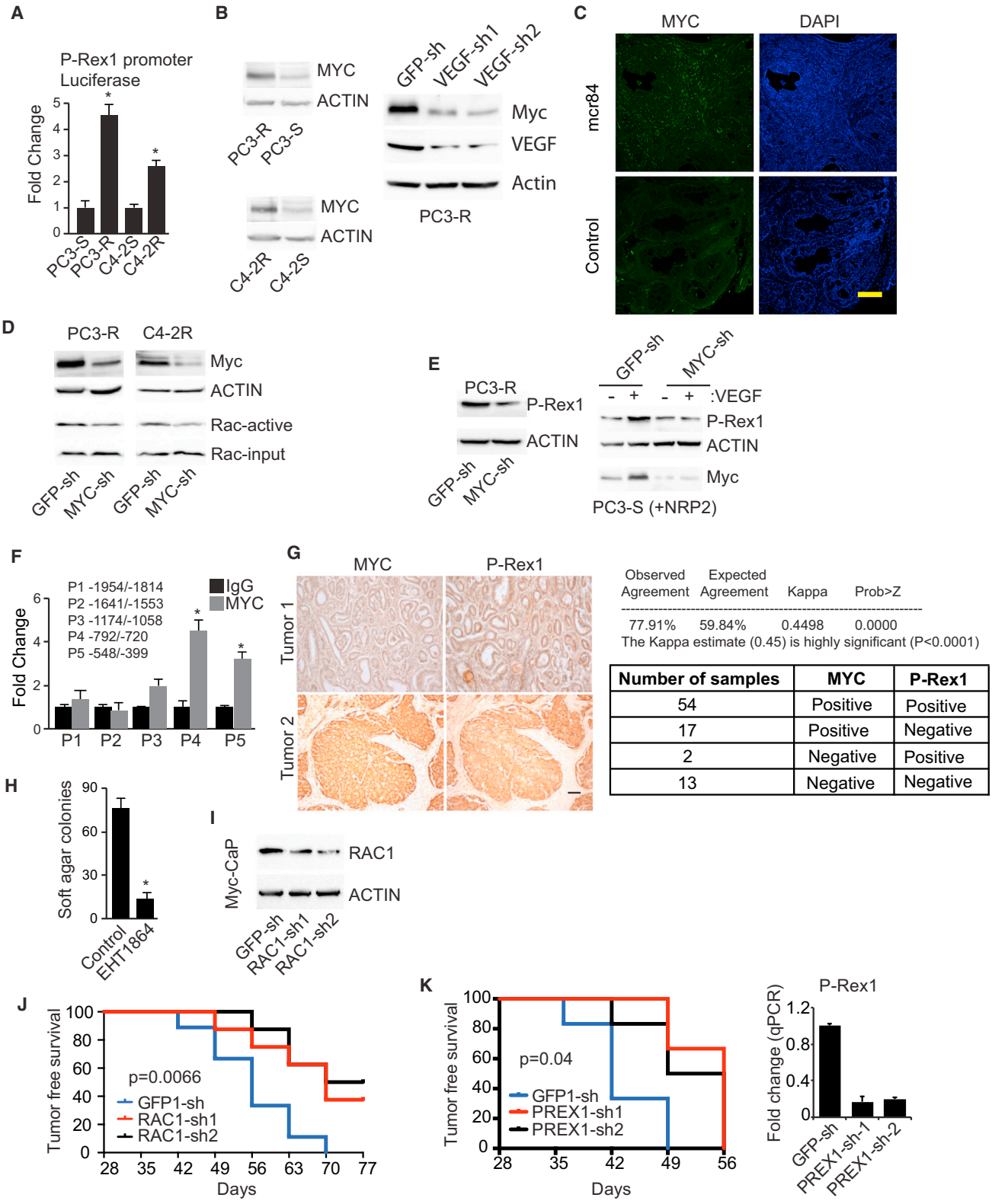

Number of samples	MYC	P-Rex1
54	Positive	Positive
17	Positive	Negative
2	Negative	Positive
13	Negative	Negative

Figure 7. Myc Regulates PREX1 Transcription in Resistant Cells

(A) A luciferase reporter construct containing the P-Rex1 promoter was expressed in sensitive and resistant PC3 and C4-2 cells, and luciferase activity was measured and normalized to Renilla.

(legend continued on next page)

of the GU tract in response to EHT1864 (Figure 4D). Targeting P-Rex1, however, may be more feasible based on our data. Nonetheless, our data demonstrate that P-Rex1/Rac1 inhibition reduces stem cell properties and renders tumor cells more sensitive to VEGF-targeted therapies.

EXPERIMENTAL PROCEDURES

Animal Studies

All mouse experiments were performed following a protocol approved by the Institutional Animal Care and Use Committee of the University of Massachusetts Medical School.

Cell Lines

PC3 (ATCC), C4-2 (UroCor), and MyC-CaP (provided by Dr. Charles L. Sawyers, Memorial Sloan-Kettering Cancer Center, New York, NY) were used. shRNA clones from the RNAi Consortium library were obtained from RNAi core, University of Massachusetts Medical School.

Cell-Based Assays

The chemosensitivity of prostate cancer cells was determined using a standard 3-(4,5-dimethylthiazol-2-yl)-2,5-diphenyltetrazolium bromide (MTT) cytotoxicity assay (Mosmann, 1983). The assay was performed 72 hr after treatment. Fluorescence-activated cell sorting was used to isolate cells based on their surface expression of CD44, CD24, and α6 and β4 integrins. The detailed procedure for isolating LSC cells from $PTEN^{pc-/-}$ mice using lineage markers (CD31, CD45, and Ter119), Sca-1, and CD49f is described previously (Mulholland et al., 2009; Lawson et al., 2007).

Isolation of Human Prostate Tumor Cells and Laser Capture Microscopy

Human prostate tumor tissue was obtained from UMASS Cancer Center Tissue Bank in compliance with the institutional review board of the University of Massachusetts Medical School. The discarded but freshly resected, prostate tumors were digested with collagenase at 37°C, and epithelial cells were isolated using an EpCaM antibody. Frozen sections were microdissected by laser capture microscopy (Arcturus PixCell 2) as described elsewhere (Goel et al., 2012) to obtain pure populations of tumor cells of defined Gleason grades. RNA was isolated from these microdissected samples using the RNeasy kit (QIAGEN), and cDNA was prepared using Superscript II reverse transcriptase (Invitrogen). Quantitative real-time PCR was done using the TaqMan assay kit (Applied Biosystems).

Promoter Activity and ChIP Assays

Prostate cancer cells were transfected with the P-Rex1 promoter luciferase construct (−2021/+3) and Renilla luciferase construct to normalize for transfection efficiency. Relative light units were calculated upon normalization with Renilla luciferase activity. ChIP assays were performed according to our published protocol (Goel et al., 2012). All ChIP experiments were repeated at least two times. The sequence of primers used to amplify the P-Rex1 promoter is provided in Figure S6G.

Statistics

Unless otherwise cited, all values are presented as the mean ± SD. For the Student's t test, comparisons between two groups were performed using two-tailed, assuming equal variance among groups. A p value less than 0.05 was considered significant. The correlation of Myc and P-Rex1 expression in human prostate cancer specimens was done using kappa statistics. The kappa estimate was tested against a null hypothesis of kappa = 0.0. For tumor-free survival xenograft experiments, the comparison between two curves was done using the log-rank (Mantel-Cox) test. All experiments were repeated at least twice with the exception of experiments involving the culture of primary tumor cells, and data from one representative experiment are shown.

SUPPLEMENTAL INFORMATION

Supplemental Information includes seven figures and can be found with this article online at http://dx.doi.org/10.1016/j.celrep.2016.02.016.

AUTHOR CONTRIBUTIONS

H.L.G. designed, executed, and analyzed experiments and wrote the manuscript. B.P. contributed to the experiments. C.W.V.K. provided NRP2 inhibitory antibody and performed plate-based inhibition assays. L.D.S. and D.L.G. provided the NSG mice. R.A.B. provided mcr84 antibody. A.M.M. supervised the study and wrote the manuscript together with H.L.G.

CONFLICTS OF INTEREST

D.L.G. is a consultant for the Jackson Laboratory. R.A.B. has a commercial research grant from Peregrine Pharmaceuticals as well as other commercial research support from Affitech and is a consultant/advisory board member of Peregrine Pharmaceuticals.

ACKNOWLEDGMENTS

Work in the authors' laboratory is supported by NIH grants CA168464 and CA159856 and by US Department of Defense prostate cancer grant W81XWH-12-1-0308 (A.M.M.), RO1GM094155 (C.W.V.K.), and Cancer Core grant CA034196 to the Jackson Laboratory (to L.D.S.). We thank Michael Lee for constructive comments on the manuscript. We also acknowledge the UMASS Medical School Cancer Center Tissue Bank for providing fresh tissue specimens and Dr. Chung-Cheng Hsieh for statistical analysis. Tissue microarrays containing prostate cancer tissues were kindly provided by Rosina Lis and Massimo Loda (Dana-Farber Cancer Institute). DNA constructs provided by other investigators are acknowledged in Experimental Procedures.

(B) Myc expression was compared between sensitive and resistant PC3 and C4-2 cells by immunoblotting (left). VEGF expression was downregulated in PC3-R cells using shRNAs, and the effect on Myc expression activation was determined by immunoblotting (right).
(C) Six-week-old $PTEN^{pc-/-}$ mice were injected (i.p.) with mcr84 (10 mg/kg) twice weekly for 3 weeks. The prostate glands were harvested and immunostained using a myc antibody.
(D) Myc expression was downregulated in resistant PC3 and C4-2 cells using shRNA, and the effect on Rac1 activation was determined.
(E) Myc expression was downregulated in PC3-R cells using shRNA, and the effect on P-Rex1 expression was determined (left). Right: NRP2-expressing PC3-S cells were transfected with either GFP-sh or Myc-sh and stimulated with VEGF (50 ng/ml) for 24 hr, and the effect on P-Rex1 and Myc expression was measured.
(F) ChIP was performed using a Myc antibody and regions of the PREX1 promoter that bound Myc were identified and quantified by qPCR.
(G) The expression of Myc and P-Rex1 was analyzed in human prostate cancer specimens by immunohistochemistry. A significant correlation of their expression was detected. The kappa estimate (0.45) is highly significant ($p < 0.0001$), and it was tested against a null hypothesis of kappa = 0.0. Scale bar, 100 μm.
(H) The ability of Myc-CaP cells to form colonies in soft agar in the presence or absence of EHT1864 was determined.
(I and J) Myc-CaP cells were transfected with two different Rac1 shRNAs, and the effect on Rac1 expression was detected by immunoblotting (I). These cells were implanted into NSG mice, and tumor onset was determined by palpation (J).
(K). Myc-CaP cells were transfected with two different P-Rex1 shRNAs, and the effect on P-Rex1 expression was quantified by qPCR (right). These cells were implanted into NSG mice, and tumor onset was determined by palpation (left).
Error bars represent mean ± SD. Bev, bevacizumab; hIgG, control immunoglobulin G. See also Figures S5–S7.

We thank Dr. Hou-Fu Guo for the plate-based inhibition data and Dr. Yaping Tu for the P-Rex1 promoter construct.

Received: September 16, 2015
Revised: December 28, 2015
Accepted: January 28, 2016
Published: February 25, 2016

REFERENCES

Baker, N.M., Yee Chow, H., Chernoff, J., and Der, C.J. (2014). Molecular pathways: targeting RAC-p21-activated serine-threonine kinase signaling in RAS-driven cancers. Clin. Cancer Res. *20*, 4740–4746.

Bid, H.K., Roberts, R.D., Manchanda, P.K., and Houghton, P.J. (2013). RAC1: an emerging therapeutic option for targeting cancer angiogenesis and metastasis. Mol. Cancer Ther. *12*, 1925–1934.

Cao, Y., Hoeppner, L.H., Bach, S., e, G., Guo, Y., Wang, E., Wu, J., Cowley, M.J., Chang, D.K., Waddell, N., et al. (2013). Neuropilin-2 promotes extravasation and metastasis by interacting with endothelial α5 integrin. Cancer Res. *73*, 4579–4590.

Chatterjee, S., Heukamp, L.C., Siobal, M., Schöttle, J., Wieczorek, C., Peifer, M., Frasca, D., Koker, M., König, K., Meder, L., et al. (2013). Tumor VEGF:VEGFR2 autocrine feed-forward loop triggers angiogenesis in lung cancer. J. Clin. Invest. *123*, 1732–1740.

Chen, X., Rycaj, K., Liu, X., and Tang, D.G. (2013). New insights into prostate cancer stem cells. Cell Cycle *12*, 579–586.

Civenni, G., Malek, A., Albino, D., Garcia-Escudero, R., Napoli, S., Di Marco, S., Pinton, S., Sarti, M., Carbone, G.M., and Catapano, C.V. (2013). RNAi-mediated silencing of Myc transcription inhibits stem-like cell maintenance and tumorigenicity in prostate cancer. Cancer Res. *73*, 6816–6827.

Colombel, M., Eaton, C.L., Hamdy, F., Ricci, E., van der Pluijm, G., Cecchini, M., Mege-Lechevallier, F., Clezardin, P., and Thalmann, G. (2012). Increased expression of putative cancer stem cell markers in primary prostate cancer is associated with progression of bone metastases. Prostate *72*, 713–720.

Craft, N., Chhor, C., Tran, C., Belldegrun, A., DeKernion, J., Witte, O.N., Said, J., Reiter, R.E., and Sawyers, C.L. (1999). Evidence for clonal outgrowth of androgen-independent prostate cancer cells from androgen-dependent tumors through a two-step process. Cancer Res. *59*, 5030–5036.

Ellwood-Yen, K., Graeber, T.G., Wongvipat, J., Iruela-Arispe, M.L., Zhang, J., Matusik, R., Thomas, G.V., and Sawyers, C.L. (2003). Myc-driven murine prostate cancer shares molecular features with human prostate tumors. Cancer Cell *4*, 223–238.

Ferrara, N. (2005). VEGF as a therapeutic target in cancer. Oncology *69* (*Suppl 3*), 11–16.

Garcia, A.J., Ruscetti, M., Arenzana, T.L., Tran, L.M., Bianci-Frias, D., Sybert, E., Priceman, S.J., Wu, L., Nelson, P.S., Smale, S.T., and Wu, H. (2014). Pten null prostate epithelium promotes localized myeloid-derived suppressor cell expansion and immune suppression during tumor initiation and progression. Mol. Cell. Biol. *34*, 2017–2028.

Geretti, E., van Meeteren, L.A., Shimizu, A., Dudley, A.C., Claesson-Welsh, L., and Klagsbrun, M. (2010). A mutated soluble neuropilin-2 B domain antagonizes vascular endothelial growth factor bioactivity and inhibits tumor progression. Mol. Cancer Res. *8*, 1063–1073.

Goel, H.L., and Mercurio, A.M. (2013). VEGF targets the tumour cell. Nat. Rev. Cancer *13*, 871–882.

Goel, H.L., Chang, C., Pursell, B., Leav, I., Lyle, S., Xi, H.S., Hsieh, C.C., Adisetiyo, H., Roy-Burman, P., Coleman, I.M., et al. (2012). VEGF/neuropilin-2 regulation of Bmi-1 and consequent repression of IGF-IR define a novel mechanism of aggressive prostate cancer. Cancer Discov. *2*, 906–921.

Goel, H.L., Pursell, B., Chang, C., Shaw, L.M., Mao, J., Simin, K., Kumar, P., Vander Kooi, C.W., Shultz, L.D., Greiner, D.L., et al. (2013). GLI1 regulates a novel neuropilin-2/α6β1 integrin based autocrine pathway that contributes to breast cancer initiation. EMBO Mol. Med. *5*, 488–508.

Gu, Y., Filippi, M.D., Cancelas, J.A., Siefring, J.E., Williams, E.P., Jasti, A.C., Harris, C.E., Lee, A.W., Prabhakar, R., Atkinson, S.J., et al. (2003). Hematopoietic cell regulation by Rac1 and Rac2 guanosine triphosphatases. Science *302*, 445–449.

Hurt, E.M., Kawasaki, B.T., Klarmann, G.J., Thomas, S.B., and Farrar, W.L. (2008). CD44+ CD24(-) prostate cells are early cancer progenitor/stem cells that provide a model for patients with poor prognosis. Br. J. Cancer *98*, 756–765.

Kelly, W.K., Halabi, S., Carducci, M., George, D., Mahoney, J.F., Stadler, W.M., Morris, M., Kantoff, P., Monk, J.P., Kaplan, E., et al. (2012). Randomized, double-blind, placebo-controlled phase III trial comparing docetaxel and prednisone with or without bevacizumab in men with metastatic castration-resistant prostate cancer: CALGB 90401. J. Clin. Oncol. *30*, 1534–1540.

Kobayashi, T., Inoue, T., Shimizu, Y., Terada, N., Maeno, A., Kajita, Y., Yamasaki, T., Kamba, T., Toda, Y., Mikami, Y., et al. (2010). Activation of Rac1 is closely related to androgen-independent cell proliferation of prostate cancer cells both in vitro and in vivo. Mol. Endocrinol. *24*, 722–734.

Lawson, D.A., Xin, L., Lukacs, R.U., Cheng, D., and Witte, O.N. (2007). Isolation and functional characterization of murine prostate stem cells. Proc. Natl. Acad. Sci. USA *104*, 181–186.

Liu, B.P., and Strittmatter, S.M. (2001). Semaphorin-mediated axonal guidance via Rho-related G proteins. Curr. Opin. Cell Biol. *13*, 619–626.

Luo, M., Fan, H., Nagy, T., Wei, H., Wang, C., Liu, S., Wicha, M.S., and Guan, J.L. (2009). Mammary epithelial-specific ablation of the focal adhesion kinase suppresses mammary tumorigenesis by affecting mammary cancer stem/progenitor cells. Cancer Res. *69*, 466–474.

Man, J., Shoemake, J., Zhou, W., Fang, X., Wu, Q., Rizzo, A., Prayson, R., Bao, S., Rich, J.N., and Yu, J.S. (2014). Sema3C promotes the survival and tumorigenicity of glioma stem cells through Rac1 activation. Cell Rep. *9*, 1812–1826.

Merino, M., Pinto, A., González, R., and Espinosa, E. (2011). Antiangiogenic agents and endothelin antagonists in advanced castration resistant prostate cancer. Eur. J. Cancer *47*, 1846–1851.

Michaelson, M.D., Oudard, S., Ou, Y.C., Sengeløv, L., Saad, F., Houede, N., Ostler, P., Stenzl, A., Daugaard, G., Jones, R., et al. (2014). Randomized, placebo-controlled, phase III trial of sunitinib plus prednisone versus prednisone alone in progressive, metastatic, castration-resistant prostate cancer. J. Clin. Oncol. *32*, 76–82.

Montalvo-Ortiz, B.L., Castillo-Pichardo, L., Hernández, E., Humphries-Bickley, T., De la Mota-Peynado, A., Cubano, L.A., Vlaar, C.P., and Dharmawardhane, S. (2012). Characterization of EHop-016, novel small molecule inhibitor of Rac GTPase. J. Biol. Chem. *287*, 13228–13238.

Mosmann, T. (1983). Rapid colorimetric assay for cellular growth and survival: application to proliferation and cytotoxicity assays. J. Immunol. Methods *65*, 55–63.

Mulholland, D.J., Xin, L., Morim, A., Lawson, D., Witte, O., and Wu, H. (2009). Lin-Sca-1+CD49fhigh stem/progenitors are tumor-initiating cells in the Pten-null prostate cancer model. Cancer Res. *69*, 8555–8562.

Parker, M.W., Hellman, L.M., Xu, P., Fried, M.G., and Vander Kooi, C.W. (2010). Furin processing of semaphorin 3F determines its anti-angiogenic activity by regulating direct binding and competition for neuropilin. Biochemistry *49*, 4068–4075.

Pentheroudakis, G., Kotoula, V., Fountzilas, E., Kouvatseas, G., Basdanis, G., Xanthakis, I., Makatsoris, T., Charalambous, E., Papamichael, D., Samantas, E., et al. (2014). A study of gene expression markers for predictive significance for bevacizumab benefit in patients with metastatic colon cancer: a translational research study of the Hellenic Cooperative Oncology Group (HeCOG). BMC Cancer *14*, 111.

Qin, J., Xie, Y., Wang, B., Hoshino, M., Wolff, D.W., Zhao, J., Scofield, M.A., Dowd, F.J., Lin, M.F., and Tu, Y. (2009). Upregulation of PIP3-dependent Rac exchanger 1 (P-Rex1) promotes prostate cancer metastasis. Oncogene *28*, 1853–1863.

Reese, D.M., Fratesi, B.S., Corry, M., Novotny, W., Holmgren, E., and Small, E.J. (2001). A Phase II Trial of Humanized Anti-Vascular Endothelial Growth

Factor Antibody for the Treatment of Androgen-Independent Prostate Cancer. Prostate J. *3*, 65–70.

Riccomagno, M.M., Hurtado, A., Wang, H., Macopson, J.G., Griner, E.M., Betz, A., Brose, N., Kazanietz, M.G., and Kolodkin, A.L. (2012). The RacGAP β2-Chimaerin selectively mediates axonal pruning in the hippocampus. Cell *149*, 1594–1606.

Ridgway, R.A., Serrels, B., Mason, S., Kinnaird, A., Muir, M., Patel, H., Muller, W.J., Sansom, O.J., and Brunton, V.G. (2012). Focal adhesion kinase is required for β-catenin-induced mobilization of epidermal stem cells. Carcinogenesis *33*, 2369–2376.

Sullivan, L.A., Carbon, J.G., Roland, C.L., Toombs, J.E., Nyquist-Andersen, M., Kavlie, A., Schlunegger, K., Richardson, J.A., and Brekken, R.A. (2010). r84, a novel therapeutic antibody against mouse and human VEGF with potent anti-tumor activity and limited toxicity induction. PLoS ONE *5*, e12031.

Tan, W., Palmby, T.R., Gavard, J., Amornphimoltham, P., Zheng, Y., and Gutkind, J.S. (2008). An essential role for Rac1 in endothelial cell function and vascular development. FASEB J. *22*, 1829–1838.

Tomić, T.T., Gustavsson, H., Wang, W., Jennbacken, K., Welén, K., and Damber, J.E. (2012). Castration resistant prostate cancer is associated with increased blood vessel stabilization and elevated levels of VEGF and Ang-2. Prostate *72*, 705–712.

Wang, K., Peng, H.L., and Li, L.K. (2012). Prognostic value of vascular endothelial growth factor expression in patients with prostate cancer: a systematic review with meta-analysis. Asian Pac. J. Cancer Prev. *13*, 5665–5669.

Wong, C.Y., Wuriyanghan, H., Xie, Y., Lin, M.F., Abel, P.W., and Tu, Y. (2011). Epigenetic regulation of phosphatidylinositol 3,4,5-triphosphate-dependent Rac exchanger 1 gene expression in prostate cancer cells. J. Biol. Chem. *286*, 25813–25822.

Zhao, J., and Guan, J.L. (2009). Signal transduction by focal adhesion kinase in cancer. Cancer Metastasis Rev. *28*, 35–49.

Zhao, D., Pan, C., Sun, J., Gilbert, C., Drews-Elger, K., Azzam, D.J., Picon-Ruiz, M., Kim, M., Ullmer, W., El-Ashry, D., et al. (2015). VEGF drives cancer-initiating stem cells through VEGFR-2/Stat3 signaling to upregulate Myc and Sox2. Oncogene *34*, 3107–3119.